

On-Demand Manipulation of Liquid Metal Droplet via van der Waals Adhesion

Jiarui Guo, Yang Wang, Xinpeng Wang, Yaowen Xing, and Liang Hu*

The actuation of liquid metal droplets is the core in the development of future liquid metal-based soft robotics or devices. In the present study, an intriguing phenomenon of actuating liquid metal droplets via van der Waals adhesion is introduced. Through the electrochemical interaction between liquid metal and nickel in an acid solution, the continuously generating hydrogen bubbles form capillary adhesion to surfaces, which provide the force bridge between two metals. Based on this mechanism, liquid metal can not only be manipulated by directly dragging a nickel rod, but also accurately and stably be driven by magnetic field due to the magnetism of nickel. In particular, the magnetic manipulation method involved in this study does not change the chemical nature of the liquid metal. With all the distinctive properties, this van der Waals force-based liquid metal actuation may offer numerous inspirations in various fields including soft robotics, flexible electronics, and microfluidics.

Gallium-based room temperature liquid metal alloys are emerging functional materials owing to their intrinsic properties, such as excellent fluidity with high surface tension, high electrical and thermal conductivity, and versatile interactions with other materials, and have drawn considerable attentions from both of academia and industry. Particularly, the deformability and mobility of liquid metals in aqueous environments allow them to be manipulated by multiple means, which has enabled diverse applications, such as soft electronics,^[1,2] soft sensors,^[3,4] stretchable circuits,^[5–8] soft robotics,^[9–11] and soft motors.^[12] Among those applications, one of the core issues is the actuation of liquid metals. Based on the source of the driving force, the driving methods can be categorized into several types. For example, the surface tension gradient force induced by electrical,^[13,14] electrochemical,^[9,12,15,16] or thermal^[17] methods can easily actuate a liquid metal droplet in

the aqueous environment. And external mechanical force from bubbles can also propel a droplet.^[9] In addition, magnetic attraction provides a favorable actuation for magnetic liquid metals with the advantages of wireless and remote control especially in an enclosed space. Several attempts to produce deformable, movable, and multifunctional magnetic liquid metals have been reported. In those studies magnetic particles such nickel,^[18] iron,^[11,19–22] and even neodymium iron boron (NdFeB)^[23] are mixed or suspended into the liquid metal to achieve magnetism. However, the rheological properties of these doped magnetic liquid metals are also altered. Generally, they become more viscoelastic and even solid like a mass of mud. Thus, the fluidity

and mobility are severely diminished. Besides, the continuous galvanic interactions within these doped magnetic materials facilitate the oxidation of the liquid gallium, which make them chemically unstable. Pure liquid metal has been reported to be quickly actuated by alternating magnetic field due to the Lorentz force. However, this actuation reported is transient and unstable in order to prevent overheating and combustion of liquid metals.^[24] These issues pose great challenges for further applications of magnetic field in liquid metal actuators. In the present study, a fundamentally new liquid metal actuation method is introduced. Here a nickel rod is observed to drag a liquid metal droplet in an acid solution which is revealed to be due to a van der Waals force-based linkage between liquid metal and nickel. Thus, liquid metal droplets can not only be dragged directly by mechanical forces, but also be driven magnetically due to the magnetism of nickel without altering the chemical nature of liquid metals. With this new method, we demonstrate the pure liquid metals can be driven on demand as movable conductors to control or repair electrical circuits. This actuation method with its unique mechanism may inspire exciting possibilities and will provide a new approach to the design of liquid metal applications.

In this study, all the results presented are operated with hydrochloric acid (HCl) solutions. All the representative results are exhibited with Galinstan droplet, while EGaIn has been shown to have similar results. Figure 1a exemplifies a 30 μL liquid metal droplet being dragged by nickel in 1 mol L⁻¹ of HCl solution (also shown in Movie S1 of the Supporting Information). Based on the preliminary studies, this actuation mode is not feasible in alkaline solutions (Figure S1, Supporting Information). Here, liquid metal droplets are exposed to nickel rods

J. Guo, Y. Wang, X. Wang, Prof. L. Hu
 Beijing Advanced Innovation Center for Biomedical Engineering
 Institute of Nanotechnology for Single Cell Analysis (INSCA)
 School of Biological Science and Medical Engineering
 Beihang University
 Beijing 100083, China
 E-mail: cnhliang@buaa.edu.cn

Prof. Y. Xing
 Chinese National Engineering Research Center of Coal Preparation and Purification
 China University of Mining and Technology
 Xuzhou 221116, China

 The ORCID identification number(s) for the author(s) of this article can be found under <https://doi.org/10.1002/admi.202000732>.

DOI: 10.1002/admi.202000732

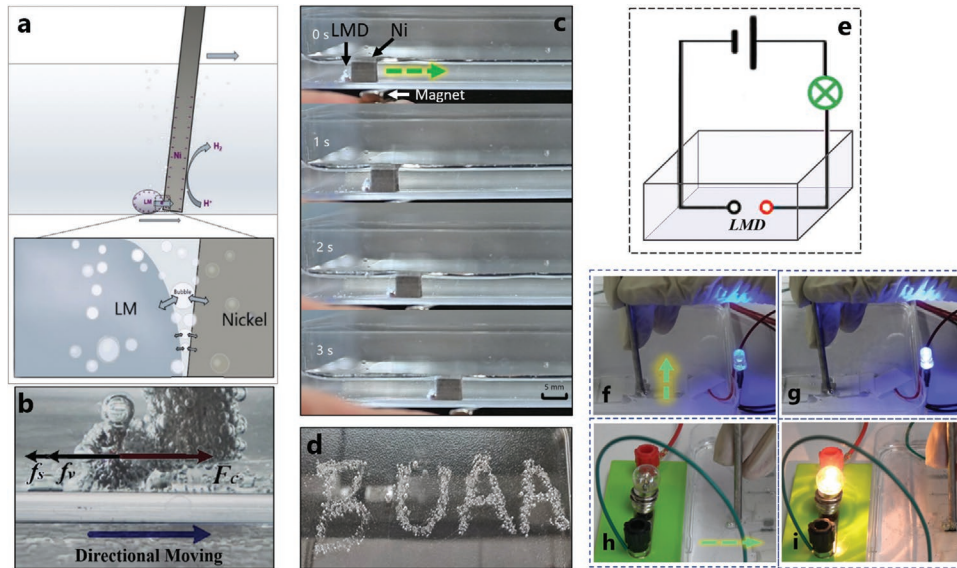
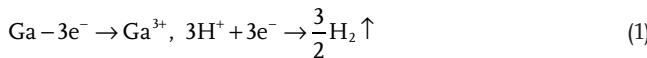


Figure 1. a) The schematic diagram of corrosive cell reaction and van der Waals adhesion of liquid metal. b) Liquid metal droplets are subject to driving forces from van der Waals adhesion, friction from the substrate, and resistance from the solution. c) The photograph of magnetically manipulating liquid metal droplet movement. d) Parts of the bubbles generated during the actuation process are adsorbed on the bottom of the container, and the specific movement path of the pattern is “BUAA.” e) The schematic illustration of the experimental design. f) The photo illustration of a conceptual experiment of actuating Galinstan droplets acting as a moving conductor of the unconnected LED circuit, g) the connected LED circuit, h) the unconnected light bulb, and i) the connected light bulb.

in HCl solution, forming a corrosion cell reaction and generating bubbles^[25]



Liquid metal droplets of the size of 30 μL can be dragged by the nickel rod at a maximum speed of 15 mm s^{-1} . Theoretically, the speed at which liquid metal droplets are pulled is governed by the resistance f_v from the solution, the frictions from the substrate f_s , and the driving force F_c (Figure 1b). When the normal acceleration of the nickel rod is greater than 30 mm s^{-2} , or when the tangential acceleration is greater than 9.6 mm s^{-2} , bubbles desorption occurs on liquid metal droplets, and the connection is broken. When the corrosion cell reaction does not occur, the liquid metal droplet and nickel are chemically stable. After recontacting, nickel will continue to drag liquid metal droplets.

Under this mechanism, the actuating process is smooth and stable. We conducted an experiment to demonstrate the magnetic manipulation of liquid metal droplets in directional motion based on this actuation mechanism. A magnet attracts a small piece of nickel that can simultaneously drag a Galinstan droplet (Figure 1c), and the droplet movement speed can easily reach more than 7 mm s^{-1} (also shown in Movie S2 of the Supporting Information). Within the speed range of mechanical dragging liquid metal droplets introduced above, the magnetic drive speed is mainly limited by the magnetic force and the friction between the nickel piece and the substrate. The liquid metal droplet can realize highly controllable motion, as demonstrated by the specific bubbles pattern of “BUAA” exhibited by the accurate Ni-drag locomotion of the liquid metal droplet and the generation of bubbles that are partially adsorbed on the container bottom surface (Figure 1d).

Furthermore, gallium-based liquid metal alloys are well known for its high electrical conductivity, and hence has been shown to have potential applications in flexible electronics. Using the driving properties proposed in this study, we can further use the Ni-drag liquid metal droplet for electronic conductor applications. Figure 1e illustrates a conceptual experiment in which Galinstan droplets work as mobile conductors (Movie S3 in the Supporting Information). A circuit pattern was sprayed on the bottom of the square petri dish, and 30 μL Galinstan droplets were placed in 0.2 mol L^{-1} HCl. HCl is a strong electrolyte in which a current can pass through. Thus, in its original state, the light emitting diode (LED) can emit faint light. At this time, the resistance between the disconnection of the circuit is 635 Ω . After the connection with the liquid metal droplets, the resistance becomes less than 0.01 Ω , and the LED light emission is enhanced. In order to achieve a stronger light and dark contrast, we chose a small resistance type bulb for testing. Under the manipulation of a nickel rod, the Galinstan droplet can be dragged to connect the gap where the circuit is broken. Then, the bulbs were lighted up. In the electrolyte solution, the circuit resistance was reduced by more than four orders of magnitude after using liquid metal droplet to connect the circuit. In other words, the liquid metal droplet is assigned here as a switch to turn on the broken circuit.

Based on the force analysis, liquid metal actuation is mainly limited by the resistance from the solution and the friction from the substrate. Therefore, the factors affecting the driving speed of the liquid metal are further studied. A series of experiments were performed by manipulating Ni with a robotic arm to quantify the actuation capability of nickel on Galinstan droplets. The liquid metal droplet is manipulated in a square polystyrene container with the length of 10 cm. And in this way, the motion state of the 30 μL actuated liquid

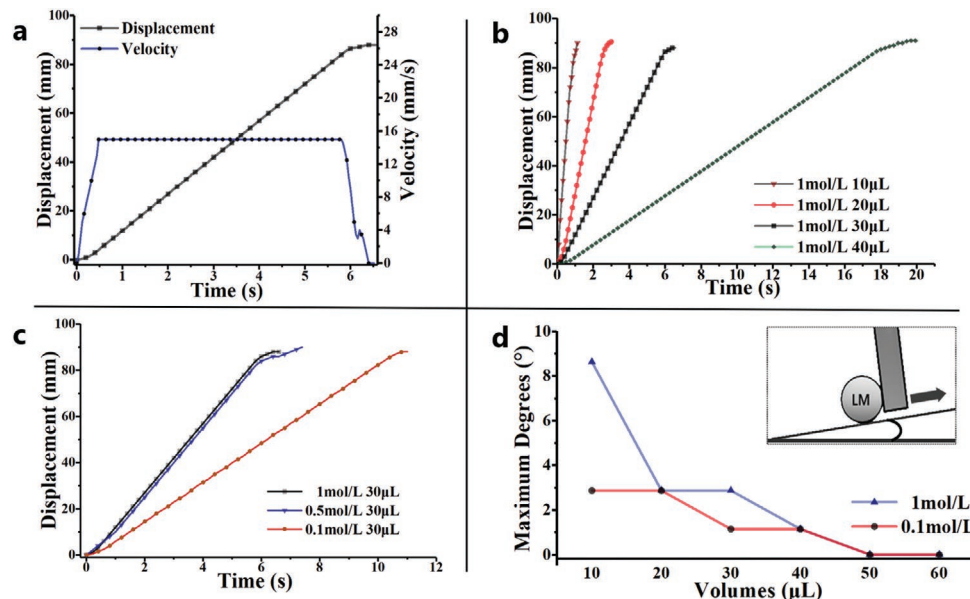


Figure 2. a) Time–displacement and time–velocity plots of the actuation process of the 30 μL Galinstan droplets in 1 mol L^{-1} HCl solution. b) Time–displacement plot of a series of Galinstan droplets of different volumes (from 10 to 40 μL —in steps of 10 μL) in 1 mol L^{-1} HCl solution. The actuation speed of liquid metal droplets is inversely proportional to the volume. c) Time–displacement plot of driving a 30 μL Galinstan droplets in a 0.1, 0.5, 1 mol L^{-1} HCl solution. In 0.5 and 1 mol L^{-1} HCl solution, the driving motion is the same. In 0.1 mol L^{-1} HCl solution, the surface oxide layer of liquid metal reduces its surface tension and increases friction. d) Line chart of the maximum climbability of Galinstan droplets with different volumes in different concentration solutions.

metal droplet introduced at the beginning of this article is recorded as **Figure 2a**. First, we set the horizontal speed of robotic arm to a relatively safe maximum speed so that the nickel rod steadily drags Galinstan droplets with a volume of 10–40 μL . **Figure 2b** shows that the speed of stable dragging decreases as the volume of the droplet increases in a solution of the same concentration. The larger volume droplet is subject to greater frictional forces from the substrate due to their heavier weight, so the traction speed of maintaining a stable drag is slow. The 10 μL Galinstan droplet can move linearly at extremely fast speeds (100 mm s^{-1}) horizontally and the speed of a 40 μL Galinstan droplet is only 5 mm s^{-1} . According to previous studies, liquid metal droplets have an oxide layer on the surface in a weakly acidic solution with pH > 0.5.^[25] Therefore, in order to investigate this actuation in different environments, we explored the difference between performances actuating with the same volume of liquid metal droplets in different concentrations of HCl solution. As shown in **Figure 2c**, in 0.5 and 1 mol L^{-1} HCl solutions, both of them are strong acid solutions that can provide excess hydrogen ions, so the same actuation situation is present. In a 0.1 mol L^{-1} HCl solution, the surface oxide layer of the liquid metal reduces its surface tension, which increases its contact area with the substrate, thereby increasing the friction force. We have also tested other solutions which can cause liquid metal to generate hydrogen bubbles. We did not observe similar on-demand manipulation in alkaline solution (0.1–2 mol L^{-1} sodium hydroxide, NaOH, solution). Based on our observation and calculation, liquid metals in alkaline solutions generally do not generate bubbles quickly and in large amounts without the addition of aluminum. We have also conducted experiments and observed

that the 0.5/1 mol L^{-1} H_2SO_4 solution and the 1 mol L^{-1} HNO_3 solution have the same effect as the HCl solution and can provide sufficient hydrogen ions. Furthermore, in order to demonstrate the motion performance of this actuation method, we performed an experiment of dragging liquid metal droplets to climb on the inclined surface. **Figure 2d** shows the maximum climbable degree of different volumes of Galinstan droplets in different concentration solutions. The process of moving on the inclined plane is subject to additional resistance provided by gravity, so the movement performance of droplets of different volumes has a large difference.

In order to macroscopically demonstrate the adhesion of nickel surface to liquid metal in acid solution, a push-and-pull method was introduced to characterize the adhesive force of nickel and other metals to Galinstan (**Figure S2**, Supporting Information). As shown in **Figure 3a**, the maximum force (637 μN) on the nickel rod is far exceeds the molybdenum (133 μN). Platinum wires, which also have good hydrogen production capacity, cause large adhesion with a small contact area. The maximum force values of tungsten and iron that hardly generate hydrogen in the experiment are too small to measure. The force (637 μN) is much smaller than the measured forces of the nickel rods that form intermetallic compounds by wetting and copper that can quickly form intermetallic compounds, both of which are 6.2–6.7 mN. The adhesive force measured on the nickel rods is large enough to drag the liquid metal droplets.

In order to find out the fundamental source of this actuation force, the following analysis and measurement are performed. Intermetallic compounds of gallium and nickel will be formed after nickel and liquid metal droplets contact for a

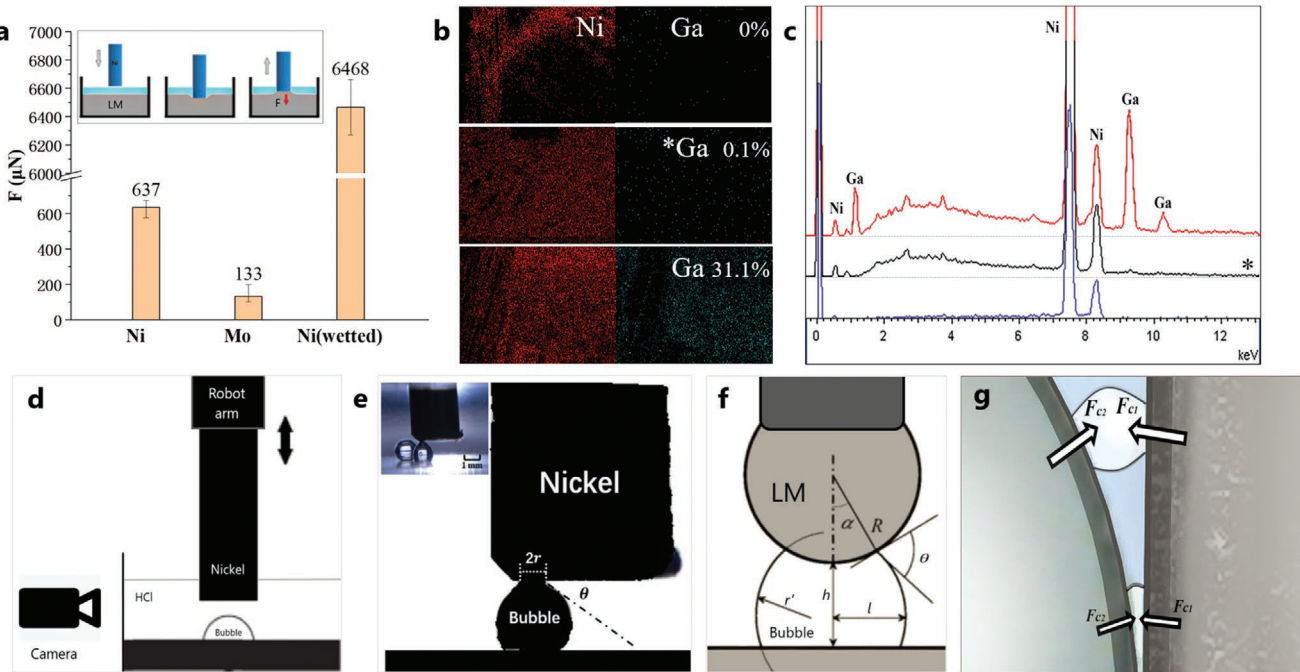


Figure 3. a) The maximum adhesion ($637 \mu\text{N}$) on nickel rods exceeds molybdenum ($133 \mu\text{N}$) and is much smaller than the measured adhesion ($6.2\text{--}6.7 \text{ mN}$) of nickel rods that form intermetallic compounds by wetting and copper that can quickly form intermetallic compounds. b) The EDX maps for the pure columnar nickel surface, the experimental columnar nickel surface, and the wetted nickel surface by liquid metal. c) The energy-dispersive X-ray spectrum, in order from bottom to top, of the pure columnar nickel surface, the experimental columnar nickel surface (marked by *), and the wetted nickel surface by liquid metal. d) The schematic diagram of an experimental device designed to determine the capillary adhesion between a metal surface and a bubble to directly observe the separation process between the metal surface and the bubble. e) The experimental photos of nickel and bubble adsorption experiments after edge recognition. The upper left corner is the original photo. f) The schematic of an experimental measurement of capillary adhesion of liquid metal droplets to hydrogen bubbles. g) The schematic diagram of van der Waals adhesion connecting liquid metal droplets to the surface of nickel in the form of a capillary bridge.

long time, which is similar to copper. Wetting and intermetallic compounds can provide a strong adhesion to the two parties involved in forming it.^[26–28] In hydrochloric acid solution, theoretically, the wettability of liquid metal to nickel and copper is different. The nickel and liquid metal form the primary battery, which produces a large number of bubbles instead of being wetted.^[29] To exactly demonstrate that the traction of nickel on gallium is driven by capillary adhesion rather than wetting and intermetallic compounds, we observed the nickel surface under electron microscope and energy spectrum, as shown in Figure 3b,c (also shown in Figure S3 of the Supporting Information). The image shows that gallium does not exist on the nickel surface, and the energy dispersive X-ray spectrometer (EDX) image shows that the surface content of gallium is less than 0.1 wt%, which is much lower than the 31.12 wt% measured by the intermetallic compound sample. The results indicate that the traction effect of nickel on liquid metal droplets is not derived from intermetallic compounds.

Some bubbles are adsorbed on the solid surface due to van der Waals force, which is also called capillary adhesion. Bubbles have been found to form bridges between nickel and liquid metal droplets, which provide the force linkage underlying mechanism similar to the froth flotation.^[30,31] In order to determine and quantify the capillary adhesion between the metal surface and the bubbles, an experimental setup was designed to directly view the detachment process between the metal surface

and the bubbles. The schematic diagram of the experimental apparatus is shown in Figure 3d, and Figure 3e is the photo of the experiment after edge recognition processing. Capillary force depends on the surface tension of the liquid–gas interface, the three-phase contact angle and the perimeter of the three-phase contact plane. It can be expressed as Equation (2)

$$F_{c1} = 2\pi r\sigma_{lg} \sin \theta \quad (2)$$

where σ_{lg} is the liquid–gas interface, r is the radius of the three-phase contact line, and θ is the contact angle between the tangents at the intersection of the bubble surface and the flat nickel surface. The above equation calculates the capillary adhesion of the nickel planar surface to the bubbles. Figure 3f is a schematic diagram for measuring the capillary adhesion of liquid metal droplets to bubbles, which can be expressed as Equation (3)

$$F_{c2} = \pi R\sigma_{lg} \sin \alpha \left[2\sin(\theta - \alpha) + R \sin \alpha \left(\frac{1}{r'} - \frac{1}{l} \right) \right] \quad (3)$$

where R is the radius of the liquid metal droplet, α is the half filling angle (measured at the particle center) of the particle–capillary bridge contact, and θ is the contact angle, measured in the liquid phase, on the particle surface. The two principal radii, r' and l , of interface curvature can be determined by

considering the simple geometry associated with the arc and the particle surface

$$r' = \frac{-R(1-\cos\alpha)+h}{\cos(\theta-\alpha)+\cos\theta} \quad (4)$$

$$l = R \sin \alpha - r'[1 - \sin(\theta - \alpha)] \quad (5)$$

The h in Equation (4) is the separation distance between the liquid metal droplet and flat surfaces. As shown in Figure 3e, the maximum capillary adhesion on the nickel surface in contact with a 0.7 mm diameter hydrogen gas bubble is 48.426 μN . The three-phase contact angle and the perimeter of the three-phase contact plane of the surface of molybdenum, tungsten, and iron in contact with hydrogen gas bubbles is small, so the capillary adhesion of it is much smaller (less than 15 μN). The maximum capillary adhesion of 30 μL Galinstan droplets fixed on a copper rod in contact with 0.5, 0.6, 0.7, 0.8 mm diameter hydrogen gas bubbles was measured and the average values were 41.72, 48.04, 51.56, 60.89 μN . Through observation and statistics, the average value of the diameter of the hydrogen gas bubbles generated during the actuation is around 0.7 mm, and around 67% of the bubble diameters are in the range of 0.55–0.8 mm. Figure 3g shows a schematic diagram of the forces F_{c1} and F_{c2} of a single bubble acting as a capillary bridge connecting a liquid metal droplet to the nickel surface. During the actual actuation, there are a number of bubbles involved in bridging the liquid metal droplets and the nickel surface. These bubbles act as force bridges to keep the liquid metal surface in contact with the nickel surface. Hydrogen bubbles are continuously generated, that is, new capillary bridges are forming and some capillary bridges may break. This is a dynamic process. Therefore, theoretical analysis and testing of the force that a single capillary bridge can provide a valuable reference for future research on the mechanical behavior caused by liquid metal van der Waals forces.

In summary, this study revealed the phenomenon of nickel actuating liquid metal droplets under the action of mechanical force or magnetism. The underlying mechanism is related to the van der Waals adhesion between nickel and liquid metal provided by the continuously forming bubble capillary bridges, which provide a fundamentally new approach in the manipulation of liquid metal droplet. At present, high-efficiency pure liquid metal actuation mostly occurs in alkaline solutions, but the acidic environment is more common in nature. Based on this mechanism, we can not only actuate liquid metal mechanically and directly, but also accurately and stably drive liquid metal droplets in a closed acidic environment using magnetic field without changing the chemical nature of liquid metals. With the expansion of knowledge about the interface of liquid metal, this van der Waals adhesion-based actuation methods may motivate more potential of liquid metal applications in the future in various fields including soft robotics and microfluidics research.

Experimental Section

Liquid metals (Galinstan consisting of 68.5 wt% gallium, 21.5 wt% indium, and 10 wt% tin, EGaIn consisting of 75.5 wt% gallium and

21.5 wt% indium), NaOH (99.99%), and HCl (37%) were commercially purchased and used as received. The HCl and NaOH electrolytes used in this study were freshly made before the experiments. Ni, Mo, W, Cu, Pt rods, wires, foils (99.95% purity) were purchased from Hebei Aoshuo Metals Co., Ltd. The magnetic field is provided by NdFeB magnets ($15 \times 5 \times 12 \text{ mm}^3$). The NdFeB magnets were purchased from Telesky Technology.

Videos were recorded using digital camcorders (Sony FDR-AX60 and Nikon Z6) to present the detailed experimental observations at about 100 fps.

The adhesion forces were measured by the dynamic contact angle measuring instrument (DCAT21).

Measurement of Capillary Adhesion of a Single Bubble: Hydrogen bubbles of different radius were fixed on a hydrophobically treated polymethyl methacrylate plate using a microsyringe. In a 1 mol L⁻¹ hydrochloric acid solution, the nickel, molybdenum, tungsten, iron, and other metals were clamped by a small mechanical arm in a vertical direction to make the bubbles contact the flat metal surface and then detach. The dynamic detachment process was captured using a 30× lens and a complementary metal oxide semiconductor (CMOS) camera when the nickel moved upward.

Surface features and chemical composition were analyzed using a scanning electron microscope equipped with an EDX (Hitachi S-4800 with EDAX).

Supporting Information

Supporting Information is available from the Wiley Online Library or from the author.

Acknowledgements

This work was supported by the 111 Project (Project No. B13003) and the National Natural Science Foundation of China (Grant No. 81801794) and the Open Laboratory Foundation of the Chinese Academy of Science (No. CRY0201915).

Conflict of Interest

The authors declare no conflict of interest.

Keywords

electrochemical interaction, liquid metals, magnetic controllability, on-demand manipulation, van der Waals adhesion

Received: April 28, 2020

Revised: June 4, 2020

Published online: June 29, 2020

- [1] S. Zhu, J.-H. So, R. Mays, S. Desai, W. R. Barnes, B. Pourdeyhimi, M. D. Dickey, *Adv. Funct. Mater.* **2013**, *23*, 2308.
- [2] J. W. Boley, E. L. White, R. K. Kramer, *Adv. Mater.* **2015**, *27*, 2355.
- [3] C. B. Cooper, K. Arutselvan, Y. Liu, D. Armstrong, Y. Lin, M. R. Khan, J. Genzer, M. D. Dickey, *Adv. Funct. Mater.* **2017**, *27*, 1605630.
- [4] W. Zhang, J. Z. Ou, S.-Y. Tang, V. Sivan, D. D. Yao, K. Latham, K. Khoshmanesh, A. Mitchell, A. P. O'Mullane, K. Kalantar-zadeh, *Adv. Funct. Mater.* **2014**, *24*, 3799.
- [5] J.-H. So, J. Thelen, A. Qusba, G. J. Hayes, G. Lazzi, M. D. Dickey, *Adv. Funct. Mater.* **2009**, *19*, 3632.

- [6] E. Palleau, S. Reece, S. C. Desai, M. E. Smith, M. D. Dickey, *Adv. Mater.* **2013**, *25*, 1589.
- [7] M. D. Dickey, *Adv. Mater.* **2017**, *29*, 1606425.
- [8] J. W. Boley, E. L. White, G. T.-C. Chiu, R. K. Kramer, *Adv. Funct. Mater.* **2014**, *24*, 3501.
- [9] J. Zhang, Y. Yao, L. Sheng, J. Liu, *Adv. Mater.* **2015**, *27*, 2648.
- [10] J. Wu, S.-Y. Tang, T. Fang, W. Li, X. Li, S. Zhang, *Adv. Mater.* **2018**, *30*, 1805039.
- [11] L. Hu, H. Wang, X. Wang, X. Liu, J. Guo, J. Liu, *ACS Appl. Mater. Interfaces* **2019**, *11*, 8685.
- [12] S. Y. Tang, V. Sivan, K. Khoshmanesh, A. P. O'Mullane, X. Tang, B. Gol, N. Eshtiaghi, F. Lieder, P. Petersen, A. Mitchell, K. Kalantar-zadeh, *Nanoscale* **2013**, *5*, 5949.
- [13] L. Sheng, J. Zhang, J. Liu, *Adv. Mater.* **2014**, *26*, 6036.
- [14] L. Hu, L. Wang, Y. Ding, S. Zhan, J. Liu, *Adv. Mater.* **2016**, *28*, 9210.
- [15] J. Ma, H. Dong, Z. He, *Mater. Horiz.* **2018**, *5*, 675.
- [16] A. F. Chrimes, K. J. Berean, A. Mitchell, G. Rosengarten, K. Kalantar-zadeh, *ACS Appl. Mater. Interfaces* **2016**, *8*, 3833.
- [17] J. B. Brzoska, F. Brochard-Wyart, F. Rondelez, *Langmuir* **1993**, *9*, 2220.
- [18] B. Ma, C. Xu, J. Chi, J. Chen, C. Zhao, H. Liu, *Adv. Funct. Mater.* **2019**, *29*, 1901370.
- [19] W. Hongzhang, Y. Bo, L. Shuting, G. Rui, R. Wei, *Mater. Horiz.* **2018**, *2*, 222.
- [20] J. Jeon, J. B. Lee, K. C. Sang, D. Kim, *Lab Chip* **2016**, *17*, 128.
- [21] F. Li, S. Kuang, X. Li, J. Shu, W. Li, S.-Y. Tang, S. Zhang, *Adv. Mater. Technol.* **2019**, *4*, 1800694.
- [22] R. Guo, X. Sun, B. Yuan, H. Wang, J. Liu, *Adv. Sci.* **2019**, *6*, 1901478.
- [23] L. Cao, D. Yu, Z. Xia, H. Wan, C. Liu, T. Yin, Z. He, *Adv. Mater.* **2020**, *32*, 2000827.
- [24] Y. Yu, E. Miyako, *iScience* **2018**, *3*, 134.
- [25] J. Tang, J. Wang, J. Liu, Y. Zhou, *Appl. Phys. Lett.* **2016**, *108*, 223901.
- [26] J. Mingear, D. Hartl, in *TMS 2017 146th Annual Meeting & Exhibition Supplemental Proc., Minerals Metals & Materials Series*, Springer, San Diego, CA **2017**, pp. 587–596.
- [27] T. Daeneke, K. Khoshmanesh, N. Mahmood, I. A. D. Castro, D. Esrafilzadeh, S. J. Barrow, M. D. Dickey, K. Kalantar-zadeh, *Chem. Soc. Rev.* **2018**, *47*, 4073.
- [28] Y. Cui, F. Liang, Z. Yang, S. Xu, X. Zhao, Y. Ding, Z. Lin, J. Liu, *ACS Appl. Mater. Interfaces* **2018**, *10*, 9203.
- [29] J. Tang, X. Zhao, J. Li, Y. Zhou, J. Liu, *Adv. Sci.* **2017**, *4*, 1700024.
- [30] A. Amirfazli, A. W. Neumann, *Adv. Colloid Interface Sci.* **2004**, *110*, 121.
- [31] T. T. Chau, W. J. Bruckard, P. T. L. Koh, A. V. Nguyen, *Adv. Colloid Interface Sci.* **2009**, *150*, 106.